Application of Continuous Time Random Walks to Transport in Porous Media†

Gennady Margolin and Brian Berkowitz*

Department of Environmental Sciences and Energy Research, Weizmann Institute of Science, Rehovot 76100, Israel

Received: October 19, 1999; In Final Form: January 10, 2000

The behavior of chemical species as they migrate through heterogeneous porous media is considered. The so-called "anomalous" transport patterns frequently measured in these materials are quantified in the framework of a continuous time random walk (CTRW) formalism. The physical basis for application of the CTRW is discussed, and new solutions for the first passage time distribution are presented to cover the entire range of transport behaviors. Application of these solutions to analysis of experimental data is also discussed.

1. Introduction

The importance of studying chemical transport in geological formations is well recognized in the context of contaminant migration in groundwater systems, oil and gas flow in petroleum reservoirs, and assessment of radioactive and toxic industrial wastes that might escape from underground repositories. The challenge in modeling these systems lies in the fact that natural heterogeneities have irregular morphologies and exist over many length scales; these heterogeneities control both the hydraulic and the chemical properties of the formation. Moreover, because of the difficulty in measuring these properties in the subsurface, only limited data, often of low reliability, are available.

There exist a variety of modeling approaches that attempt to predict the spatial and temporal migration of chemical species—either conservative or reactive—in geological formations. Most of these approaches are based on various deterministic[1] and stochastic[2] forms of the so-called advection-dispersion equation (ADE). Laboratory and field-scale application of this equation is based on the assumption that dispersion (plume spreading) behaves macroscopically as a Fickian diffusive process, with the macrodispersivity being assumed constant in space and time. However, laboratory, field, and Monte Carlo analyses have demonstrated that dispersivity is not constant and is in fact dependent on the time and/or length scale of measurement. This finding, often called the "scale effect", is what we denote "anomalous transport". In fact, given its ubiquity, such transport should be considered the norm.

In this paper we discuss a method, based on a continuous time random walk (CTRW) formalism, that is inherently suited to characterizing and quantifying anomalous transport. This formalism was first used by Scher and Lax[3,4] to calculate impurity conduction in semiconductors and by Montroll and Scher[5] and Scher and Montroll[6] in conjunction with studies of amorphous semiconductors. They considered charge carriers moving through or being trapped by random sites in solids. In the framework of porous and fractured geological formations, the CTRW theory has already been applied by Berkowitz and Scher[7] and by Berkowitz et al.[8] to quantify chemical transport. These studies demonstrated the relevance and effectiveness of the CTRW approach by analyzing numerical simulations and laboratory and field measurements. We note that while our emphasis here is on geological media, the CTRW approach is generally applicable to modeling transport phenomena in any heterogeneous material.

In section 2 we consider the physical behavior of conservative chemical species migrating in heterogeneous porous materials, starting from a basic, intuitive model of tracer advection. Section 3 presents some known results and interprets them in the context of the present work. We expand theoretical developments for some important classes of heterogeneity and discuss how the theory can be compared to data from laboratory and field experiments in section 4. We then return, in section 5, to consideration of a general physical picture of chemical migration over increasing length scales.

2. Physical Arguments for the CTRW Theory

We consider transport of a conservative chemical species (tracer) migrating through a (fully or partially) water-saturated geological formation. Heterogeneities in the formation may consist of fractures and/or lenses of porous rocks with different mineralogy (e.g., quartz, clay, carbonates). The physical picture with which we start is very simple: under an applied external pressure gradient, the velocity and flux distributions of the carrier liquid (water) are determined by the structure of the heterogeneities, as well as by the liquid properties. "Particles" representing the chemical species move with the carrier liquid through the medium via different paths having spatially changing velocities. Different paths are traversed by different numbers of particles.

This transport can in general be represented by a coupled probability function that describes particle "transitions" over given distances, in given directions, and in given times.[3,7] By coupling particle migration in space and time, such a function naturally accounts for particle transitions that extend over short and long distances, and over short and long times. Note that the magnitudes of these transition times and distances are not necessarily correlated. If, however, the medium is considered as a "black box", more phenomenological approaches that do not explicitly use the natural characteristic lengths of the medium can be applied. Thus, one can consider the distribution of transition lengths for a fixed time interval, or the distribution of times for a fixed transition length. In the present paper we start with the latter approach and then show that it is, in fact, mathematically equivalent to the general coupled description.

If one follows the movement of tracer particles in the medium, one can divide the path of each particle into equidistant

† Part of the special issue "Harvey Scher Festschrift".

* Corresponding author.

10.1021/jp993721x CCC: $19.00
Published on Web 03/09/2000

"displacements" (or "transitions") in the mean flow direction, and determine the distribution of times for a transition. We denote by $\psi(t)dt$ the probability that a particle entering a displacement interval at time zero will just reach the end of it in the time interval $[t, t + dt)$. For meaningful determination of $\psi(t)\ dt$, some kind of averaging must be applied: the medium (which is assumed to be a stationary, heterogeneous one) is divided into a large number of intervals and/or a sufficient number of tracer particles is introduced and/or a sufficient number of realizations of the medium is used. In mildly heterogeneous media, the displacement time density function $\psi(t)$ will decrease rapidly for large times, and its first and second moments will exist. We note that the time measure of "short" and "long" can be compared to, for example, the arrival time of half of the tracer particles at a measurement plane (outlet), denoted t_r. By the central limit theorem, the existence of the first two moments of $\psi(t)$ guarantees that the arrival time distribution (hereafter referred to as the first passage time distribution, or FPTD) will be Gaussian. However, in highly heterogeneous media of finite size, situations can arise wherein the second and even the first moments are effectively infinite (i.e., not small compared to t_r^2 and t_r). This gives rise to anomalous transport.

The hallmark of anomalous transport lies in the asymptotic (long time) behavior of $\psi(t)$. In general, only two simple asymptotic forms of $\psi(t)$ can exist: exponential or algebraic decay. Adoption of an exponential form, however, necessarily leads to Gaussian transport. Thus, when considering non-Gaussian transport behaviors, it is relevant to approximate the long time behavior of $\psi(t)$ as $\psi(t) \sim t^{-1-\beta}$ (see refs 5−7). While any asymptotic decay behavior can be formulated as an algebraic decay with a changing β, it is reasonable to assume (as we discuss below) that β changes only very slowly with the length scale in highly heterogeneous systems.

Even in the simplest case of water and tracer flowing through a tube or between parallel plates, anomalous (non-Gaussian) transport (with $\beta = 1$) would arise if there were no diffusion (mixing) among strata with different velocities. To illustrate this point, consider a parabolic velocity profile, in a section of a cylindrical tube of length L and radius R. The velocity at any radius r within the tube is $v(r) = v_0(1 - r^2/R^2)$, where v_0 is the maximum velocity, so that $2r\ dr = -R^2\ dv/v_0$. The number of particles moving with the same velocity and thus arriving in the same time is $dN = 2\pi r\ dr\ n$, where $N_0 = \pi R^2 n$ is the total number of particles. If by zero time we define the arrival time of the fastest particles then the arrival time can be written as $t = L/v - L/v_0$, i.e., $dv = -L\ dt/(t + L/v_0)^2$. Substitution of the above expressions for $2r\ dr$ and dv into the expression for dN yields $dN = LN_0\ dt/v_0(t + L/v_0)^2 \sim dt/t^2$ for large t, which indicates $\beta = 1$. Similar analysis for flow between parallel plates gives the same result. Obviously, in reality such behavior can be observed only for sufficiently large v_0 and/or for a sufficiently short tube. Transport patterns in porous media are affected by advection, at both large and small length scales, as well as by diffusion on smaller scales. While diffusion effects cannot be ignored, transport analogous to that in a tube (with no diffusion) can occur on a much larger scale because the complex pore space morphology in rock materials can lead to formation of preferential flow paths with limited mixing. In general, the interplay of mixing and spreading mechanisms at different scales can lead to anomalous transport.

We consider now, more generally, the influence of the exponent β. It is clear that $\beta > 0$, since $\int_0^\infty \psi(t)\ dt = 1$. For $\beta > 2$ the first two moments of $\psi(t)$ exist and thus the evolution of a tracer plume will display Gaussian behavior. If $1 < \beta < 2$, the second moment of $\psi(t)$ is divergent, while for $\beta < 1$ the mean time for a displacement is also infinite. Distributions having such an algebraic tail with $0 < \beta < 2$ are called Lévy distributions (see ref 10). These distributions are unique in that the distribution of the sum of Lévy variables (having the same β) will have the same long tail. This property is analogous to that of Gaussian distributions, wherein the sum of Gaussian variables is also Gaussian.

Shlesinger[9] has shown that for $\beta < 1$, $\langle l(t)\rangle \sim \sigma(t) \sim t^\beta$, where $\langle l(t)\rangle$ is the mean displacement of the particle plume, as a function of time and $\sigma(t)$ is its standard deviation. Since the ratio $\sigma(t)/\langle l(t)\rangle$ is constant in this case, the FPTD curves are similar on different spatial scales. There is no relative narrowing of the plume distribution with growing scale: this universality property[6] can explain the growth of dispersivity with scale (as noted in the Introduction).

For $1 < \beta < 2$ it was shown[9] that $\langle l(t)\rangle \sim t$ while $\sigma(t) \sim t^{(3-\beta)/2}$, hence $\sigma(t)/\langle l(t)\rangle \sim t^{(1-\beta)/2}$. In this case the mean transition time is finite, so that the time distribution becomes narrower, in relative terms, with growing length scales. There is no universality but the relative narrowing of the FPTD curve is slower than in the Gaussian case, forcing the effective dispersivity to grow. It is well-known that for a Gaussian distribution, $\langle l(t)\rangle \sim t$, $\sigma(t) \sim t^{1/2}$, and $\sigma(t)/\langle l(t)\rangle \sim t^{-1/2}$.

3. FPTD for $\beta < 1$

Anomalous transport for the case $\beta < 1$ was first investigated by Montroll and Scher[5] and by Scher and Montroll.[6] The FPTD function $f(\tau)$ for a pulse injection, where τ is some nondimensional time (to be discussed below), derived by Scher and Montroll[6], is

$$\tau f(\tau) = -\frac{1}{\pi}\sum_{n=0}^{\infty}\left(-\frac{l}{\tau^\beta}\right)^n \frac{\Gamma(n\beta+1)}{\Gamma(n+1)}\sin \pi\beta n \qquad (1)$$

where l is the distance traversed by particles, in units of the displacement (transition) length. It was also shown[6] that

$$\tau f(\tau) \simeq \frac{\exp\{-[(1-\beta)/\beta](\beta l/\tau^\beta)^{1/(1-\beta)}\}}{[2\pi(1-\beta)(\tau^\beta/\beta l)^{1/(1-\beta)}]^{1/2}}, \qquad \frac{l}{\tau^\beta} \gg 1 \quad (2)$$

When using this solution, one assumes that tracer particles are spread, initially, with constant density over the inlet face (perpendicular to the flow direction) of the domain, or that the domain is sufficiently long such that the effect of the initial tracer distribution is negligible.

From eqs 1 and 2 it is clear that the cumulative FPTD curve is a function of $\tau/l^{1/\beta}$, where both τ and l are nondimensional variables. These variables must be defined in terms of variables from field and/or laboratory measurements. Berkowitz et al.[8] define $\tau \equiv \bar{v}t/\langle l\rangle$ where $\bar{v}$ is some characteristic flow velocity and $\langle l\rangle$ is a single transition length. As mentioned above, for $\beta < 1$, the mean particle displacement $\langle l(t)\rangle$ scales as t^β and thus the mean particle velocity will decrease with time or distance as $t^{\beta-1} \sim \langle l(t)\rangle^{1-1/\beta}$. Since all cumulative FPTD curves reach a half concentration breakthrough at $\tau/l^{1/\beta} \approx 1$, Berkowitz et al.[8] use a formula similar to

$$t_r \cong \frac{\langle l\rangle}{\bar{v}}\left(b_\beta \frac{L}{\langle l\rangle}\right)^{1/\beta} \qquad (3)$$

where L is the distance from inlet to outlet. In their case, $b_\beta = 1$.

When $\beta < 1$, there arises a question of how to define units of time, since the mean time is infinite. By introducing the time unit as $\langle l\rangle/\bar{v}$, some velocity $\bar{v}$ is chosen. This velocity defines the coefficient of the long time behavior of $\psi[t(\tau)]$ and thus specifies the coefficient b_β in its Laplace transform (see ref 6 and also section 4). In this way, $\bar{v}$ can be chosen such that $b_\beta = 1$ but, in general, b_β will appear in (3). From (3) it follows that if $\bar{v}$ is kept constant, and since t_r and L are constants for a given experiment, then

$$\langle l\rangle^{\beta-1} b_\beta = \text{const} \tag{4}$$

for different choices of the single transition length $\langle l\rangle$.

We observe that the quantity $v_{\langle l\rangle} \equiv \bar{v}/b_\beta^{1/\beta} \sim \langle l\rangle^{1-1/\beta}$ can be interpreted as the mean particle velocity for a given distance $\langle l\rangle$, in agreement with the discussion above (see also discussion regarding Figure 3, below). When a particular $\langle l\rangle$ is chosen, then τ is linearly proportional to t. The coefficient of proportionality can be determined by translating the theoretical cumulative FPTD curve along the (temporal) x-axis to fit the experimental measurements.

4. FPTD for $\beta > 1$

4.1. Mathematical Development for $1 < \beta < 2$. Development of the FPTD solution for $1 < \beta < 2$ is similar to that given in Scher and Montroll[6] for the case $0 < \beta < 1$. In the present case, the leading terms of the Laplace transform $\psi^*(u)$ of the transition time density function $\psi(t)$, which decreases as $t^{-1-\beta}$ for $t \to \infty$, can be written for small u as

$$\psi^*(u) \approx 1 - \langle t\rangle u + c_\beta u^\beta \approx \mathrm{e}^{-\langle t\rangle u + c_\beta u^\beta} \tag{5}$$

where c_β is a positive coefficient and $\langle t\rangle$ is a mean transition time.

Using our definition of $\psi(t)$, we show here briefly how the FPTD at a distance of l transitions from the inlet can be obtained. This FPTD is the distribution of the sum of l random variables (times), each of which follows the probability density function $\psi(t)$. It is well-known that the distribution of the sum of random variables is the convolution of their distributions. Thus, by the properties of the Laplace transform L,

$$\text{FPTD} = L^{-1}\{[\psi^*(u)]^l\} \tag{6}$$

Here and in the remainder of the text, we suppress explicit dependence of the FPTD on time t, since t is not always written explicitly in the right-hand sides of the equations but is implicit through other variables.

Introducing the nondimensional time $\tau \equiv t/\langle t\rangle$ and the nondimensional Laplace variable $s = u\langle t\rangle$, we can write using (5) the first passage time distribution as

$$\text{FPTD} = \frac{1}{2\pi\mathrm{i}\langle t\rangle}\int_{c-\mathrm{i}\infty}^{c+\mathrm{i}\infty} \mathrm{d}s\, \mathrm{e}^{s(\tau-l)+lb_\beta s^\beta} \tag{7}$$

where $b_\beta \equiv c_\beta/\langle t\rangle^\beta$. For the two cases $\tau < l$ and $\tau > l$, with $\nu \equiv |\tau - l|$, (7) can be rewritten as

$$\text{FPTD} = \frac{1}{2\pi\mathrm{i}\langle t\rangle}\int_{c-\mathrm{i}\infty}^{c+\mathrm{i}\infty} \mathrm{d}s\, \mathrm{e}^{gs^\beta}\sum_{n=0}^{\infty}\frac{(\pm s\nu)^n}{n!} \tag{8}$$

where $g \equiv lb_\beta$ and "+" corresponds to $\tau > l$.

For each n in (8), we have a term

$$\begin{aligned} I_n &\equiv \frac{\nu^n}{2\pi\mathrm{i}\langle t\rangle n!}\int_{c-\mathrm{i}\infty}^{c+\mathrm{i}\infty} \mathrm{d}s\, \mathrm{e}^{gs^\beta} s^n \\ &= \frac{\nu^n}{2\pi\mathrm{i}\langle t\rangle n!\beta g^{(n+1)/\beta}}\int_{c_\xi} \xi^{(n+1-\beta)/\beta}\mathrm{e}^{\xi}\,\mathrm{d}\xi \\ &= \frac{\nu^n}{\langle t\rangle n!\beta g^{(n+1)/\beta}}\frac{1}{\Gamma\left(1-\dfrac{n+1}{\beta}\right)} \\ &= \frac{\nu^n}{\pi\beta\langle t\rangle g^{(n+1)/\beta}}\frac{\Gamma\left(\dfrac{n+1}{\beta}\right)}{\Gamma(n+1)}\sin\frac{\pi(n+1)}{\beta} \end{aligned} \tag{9}$$

where first we replaced the variable $\xi \equiv gs^\beta$ (which is allowed since the negative part of the real axis is a branch cut) and c_ξ denotes a contour of integration in the complex plane. The resulting integral is a known representation of the Γ function. In the last step the two well-known relations $n! \equiv \Gamma(n+1)$ and $\Gamma(z)\,\Gamma(1-z) = \pi/\sin\pi z$ were used. The resulting solution can be evaluated numerically only for small ν. For large ν other expansions are developed below.

Consider the case $\tau \gg l$. Then we define a small parameter $\gamma \equiv g/\nu^\beta$, and if $r \equiv s\nu$ then

$$\begin{aligned} \text{FPTD} &= \frac{1}{2\pi\mathrm{i}\nu\langle t\rangle}\int_{c-\mathrm{i}\infty}^{c+\mathrm{i}\infty} \mathrm{d}r\, \mathrm{e}^{r+\gamma r^\beta} \\ &= \frac{1}{2\pi\mathrm{i}\nu\langle t\rangle}\int_{c-\mathrm{i}\infty}^{c+\mathrm{i}\infty} \mathrm{d}r \sum_{n=0}^{\infty}\frac{(\gamma r^\beta)^n}{n!} \\ &= \frac{1}{\nu\langle t\rangle}\sum_{n=0}^{\infty}\frac{\gamma^n}{\Gamma(n+1)\Gamma(-\beta n)} \\ &= \frac{-1}{\pi\nu\langle t\rangle}\sum_{n=0}^{\infty}\gamma^n\frac{\Gamma(\beta n+1)}{\Gamma(n+1)}\sin\pi\beta n \end{aligned} \tag{10}$$

In the limit of $1 \ll \tau \ll l$ the method of steepest descent can be applied as follows: we define $h \equiv (l-\tau)/g^{1/\beta}$. For small τ, $h \sim l^{1-1/\beta} \to \infty$ as $l \to \infty$ so h is large. The first passage time distribution can be written as (see (7))

$$\text{FPTD} = \frac{1}{2\pi\mathrm{i}\langle t\rangle\beta g^{1/\beta}}\int_{c_\xi} \xi^{(1-\beta)/\beta}\mathrm{e}^{\xi - h\xi^{1/\beta}}\,\mathrm{d}\xi \tag{11}$$

which is close in form to the expression in Scher and Montroll,[6] for which the steepest descent method was used. Using this method, we obtain

$$\text{FPTD} = \frac{\left(\dfrac{h}{\beta}\right)^{(2-\beta)/[2(\beta-1)]}}{g^{1/\beta}\langle t\rangle(2\pi\beta(\beta-1))^{1/2}}\exp\left\{-(\beta-1)\left(\frac{h}{\beta}\right)^{\beta/(\beta-1)}\right\} \tag{12}$$

As developed above, for τ near l the following can be used:

$$\text{FPTD} = \frac{1}{\pi\beta\langle t\rangle g^{1/\beta}}\sum_{n=0}^{\infty}(-h)^n\frac{\Gamma\left(\dfrac{n+1}{\beta}\right)}{\Gamma(n+1)}\sin\frac{\pi(n+1)}{\beta} \tag{13}$$

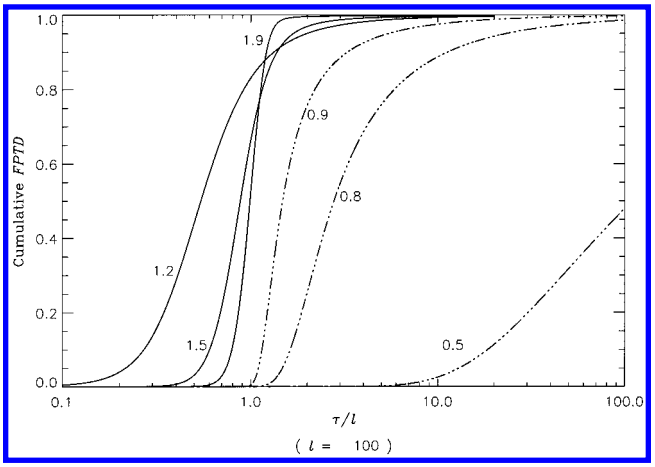

Figure 1. Cumulative first passage time distributions for $l = 100$, $b_\beta = 1$ and different values of β (labeled near the corresponding curves). The two regimes $1 < \beta < 2$ and $\beta < 1$ are shown by solid and broken curves, respectively.

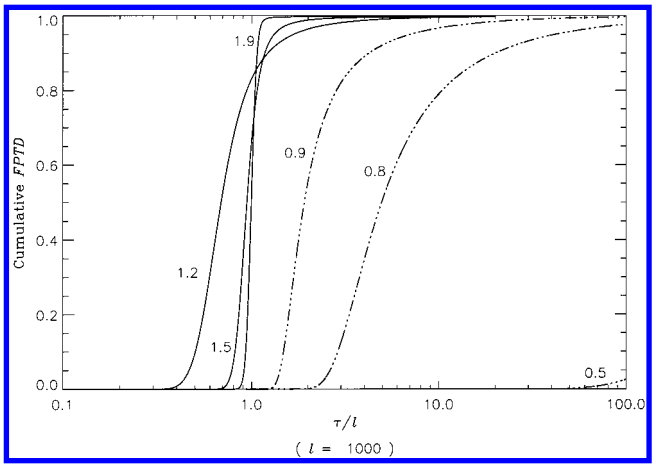

Figure 2. Cumulative first passage time distributions for $l = 1000$, $b_\beta = 1$ and different values of β (labeled near the corresponding curves). The two regimes $1 < \beta < 2$ and $\beta < 1$ are shown by solid and broken curves, respectively.

and for $\tau \gg l$

$$\mathrm{FPTD} = \frac{1}{\pi\langle t\rangle g^{1/\beta} h}\sum_{n=0}^{\infty}(-h)^{-n\beta}\frac{\Gamma(\beta n+1)}{\Gamma(n+1)}\sin\pi\beta n \quad (14)$$

Some cumulative FPTD's based on the above solutions are shown in Figures 1 and 2. The solutions (12)−(14) for the ranges $\tau \ll l$, $\tau \approx l$, and $\tau \gg l$, respectively, are combined to yield these curves. We see that while the curves with $\beta > 1$ are distributed around $\tau/l = 1$, the curves with $\beta < 1$ start at longer times for smaller values of β and approach $\tau/l = 1$ when β is close to 1. To explain this behavior, recall that $l = L/\langle l\rangle$, where L is the domain length and $\langle l\rangle$ is a single displacement length. In the case $1 < \beta < 2$, we have $\tau \equiv t/\langle t\rangle$, and since $\langle l\rangle = v\langle t\rangle$, where v is the mean tracer velocity, equal to the mean carrier velocity, it follows that $\tau/l = tv/L$, independent of $\langle l\rangle$. For $\beta < 1$ we obtain $\tau/l = tv_{\langle l\rangle}/L$, where $v_{\langle l\rangle}$ is the effective tracer velocity at distance $\langle l\rangle$. If considered for the same times and domain length, the curves presented in Figures 1 and 2 apply to the case $v_{\langle l\rangle} = v$; i.e., the effective tracer velocities (for $\beta < 1$) for the distance $\langle l\rangle$ are equal to the mean carrier velocity for the cases $1 < \beta < 2$. Recalling that for $\beta < 1$ the mean particle velocity decreases with distance (see discussion in section 3), it therefore follows that the effective tracer velocity (for $\beta < 1$) for the distance L will be less than v. Note also that the decrease is faster for smaller β (section 3). This feature explains why curves with $\beta < 1$ begin rising later.

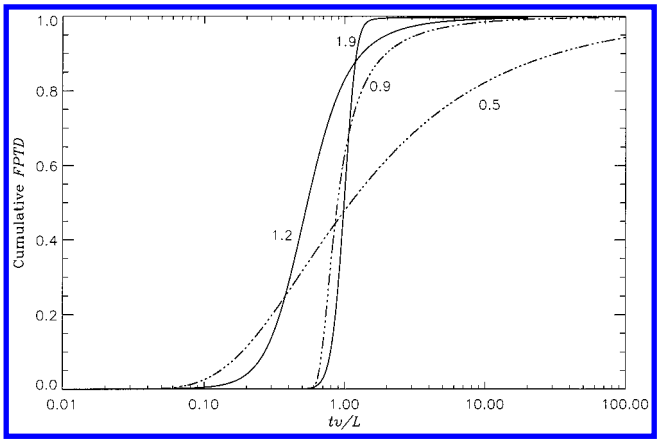

Figure 3. Cumulative first passage time distributions for $v_L = v$ and different values of β (labeled near the corresponding curves). For the $1 < \beta < 2$ cases, $b_\beta = 1$ and $l = 100$. The two regimes $1 < \beta < 2$ and $\beta < 1$ are shown by solid and broken curves, respectively.

Comparing Figures 1 and 2, we note that curves with $\beta > 1$ become more compact for longer distances, which is similar to Gaussian behavior. In contrast, curves with $\beta < 1$ spread even more. This is because of universality and because the effective velocity of the tracer decreases even further for longer distances. Also we mention here that Gaussian FPTD curves will be symmetrically distributed with respect to the line $\tau/l = 1$, while curves with $\beta < 2$ are asymmetric.

Figure 3 presents cumulative FPTD distributions for the case $v_L = v$, where v_L is the effective tracer velocity for the full domain length. In this case, a direct comparison of the curves is possible, and several interesting features can be noted. Significantly, the tail of late particle arrival times lengthens as β decreases. In contrast, however, the other sections of the FPTD curves, i.e., the early and "bulk" arrival times, do not follow a consistent progression with decreasing β.

4.2. Comparison of FPTD Curves to Data. Now we consider the question of fitting theoretical curves to experimental measurements, for a known value of β in the range $1 < \beta < 2$. The mean (tracer and carrier) velocity v is assumed known from the measurements. Note that the family of curves having the same β, but with other free parameters being variable, is analogous to a Gaussian distribution form. Fitting of these curves to measurements requires determination of one parameter, denoted below as A; fitting of this parameter is similar, in some sense, to determining the dispersion coefficient of a Gaussian distribution. First, using (13), which is the exact solution, we calculate the cumulative FPTD:

$$\mathrm{FPTD}_{\mathrm{tot}}(t) \equiv \int_0^t \mathrm{FPTD}(t')\,\mathrm{d}t'$$

$$= \int_{(L/\langle l\rangle)^{1-1/\beta}(1/b_\beta^{1/\beta})(1-vt/L)}^{(L/\langle l\rangle)^{1-1/\beta}(1/b_\beta^{1/\beta})} \frac{\mathrm{d}h}{\pi\beta}\sum_{n=0}^{\infty}(-h)^n \times \frac{\Gamma\left(\frac{n+1}{\beta}\right)}{\Gamma(n+1)}\sin\frac{\pi(n+1)}{\beta} \quad (15)$$

where, as defined above, $g = lb_\beta$ and $\mathrm{d}t = \langle t\rangle\,\mathrm{d}\tau = -\langle t\rangle g^{1/\beta}\,\mathrm{d}h$. We see that the cumulative FPTD for given time, velocity, and domain length depends only on the limits of the integral. Also,

the result cannot depend on our choice of $\langle l \rangle$. The only possible conclusion then is that the integral limits are independent of $\langle l \rangle$, i.e., (cf. (4)),

$$\langle l \rangle^{\beta - 1} b_\beta = \text{const} \tag{16}$$

From the definition of h,

$$h = \frac{L - vt}{\langle l \rangle^{1-1/\beta} (L b_\beta)^{1/\beta}} \equiv \frac{L - vt}{A} \tag{17}$$

where A is the unknown constant to be determined. We know that when $t = L/v$, $h = 0$ and from (13)

$$\text{FPTD}_{|h=0} = \frac{v\,\Gamma(1/\beta) \sin\frac{\pi}{\beta}}{\pi\beta \langle l \rangle^{1-1/\beta} (L b_\beta)^{1/\beta}} \equiv \frac{v\,\Gamma(1/\beta) \sin\frac{\pi}{\beta}}{\pi\beta A} \tag{18}$$

The left-hand side of (18) can be determined directly from the experimental data. Then the value of A is known and, by using (17) together with (12)−(14), the theoretical curves can be fit to the measurements.

It is important to stress here that because of the similarity of the curve shapes for different β (see Figures 1−3), and because β is not usually known a priori, determination of a "true" β requires at least two sets of FPTD measurements at different distances from the source. Then β can be estimated from the rate of relative narrowing of the distribution with length. Also, with two sets of measurements, it is possible to determine whether there is a decrease in tracer velocity; in such a case, we must have $\beta < 1$. Moreover, from the rate of the decrease, β can be estimated.

4.3. FPTD for $\beta > 2$. We now demonstrate that when $\beta > 2$, Gaussian behavior arises, in accordance with the central limit theorem. Indeed, in this case the leading terms of $\psi^*(u)$ for small u (i.e., for long times) will be $\psi^*(u) \approx 1 - \langle t \rangle u + \langle t^2 \rangle u^2/2$. Comparing this expansion to (5), we see that to obtain the FPTD we can set $\beta = 2$ in the formulas (12)−(14). Recalling that $g = l b_\beta$ and $l = L/\langle l \rangle$, and that in this case $b_\beta = \langle t^2 \rangle/(2\langle t \rangle^2)$, (12) will transform into

$$\begin{aligned} \text{FPTD} &= \frac{1}{g^{1/2} \langle t \rangle 2\sqrt{\pi}} \exp\left\{ -\frac{(l - \tau)^2}{4g} \right\} \\ &= \sqrt{\frac{v\langle t \rangle}{2\pi L \langle t^2 \rangle}} \exp\left\{ -\frac{(L - vt)^2}{2Lv\langle t^2 \rangle/\langle t \rangle} \right\} \end{aligned} \tag{19}$$

and (13) will give the same result:

$$\begin{aligned} \text{FPTD} &= \frac{1}{2\pi \langle t \rangle \sqrt{l b_\beta}} \sum_{m=0}^{\infty} h^{2m} \frac{\Gamma(m + {}^1\!/_2)}{\Gamma(2m+1)} \sin\frac{\pi(2m+1)}{2} \\ &= \frac{1}{2\pi \langle t \rangle \sqrt{l b_\beta}} \sum_{m=0}^{\infty} (-h^2)^m \frac{(2m-1)!!\sqrt{\pi}}{2^m (2m)!} \\ &= \sqrt{\frac{v\langle t \rangle}{2\pi L \langle t^2 \rangle}} \exp\left\{ -\frac{(L - vt)^2}{2Lv\langle t^2 \rangle/\langle t \rangle} \right\} \end{aligned} \tag{20}$$

while eq 14 is identically zero (i.e., no long tail).

The solutions (19) and (20) represent Gaussian behavior. We note here that the FPTD curves cannot be compared directly to concentration distributions over space: integration of a concentration distribution over *space* gives unity, while integration over *time* of an FPTD gives unity.

Finally, from the scaling relation (16), and with $\beta = 2$, it follows that

$$b_{\beta>2} \equiv \frac{\langle t^2 \rangle}{2\langle t \rangle^2} = \frac{\text{const}}{\langle l \rangle} \tag{21}$$

or

$$\langle t^2 \rangle \sim \langle l \rangle \tag{22}$$

where now $\langle l \rangle$ is any distance where the FPTD is measured and $\langle t^2 \rangle$ is the second moment of this FPTD distribution. At longer distances the relative time spread $\langle t^2 \rangle/\langle t \rangle^2$ decreases as $1/\langle l \rangle$. We mention that the ratio $\langle t^2 \rangle/\langle t \rangle$ is constant, independent of our choice of $\langle l \rangle$, as must also follow from (19) and (20). This is analogous to the behavior of the spatial moments with time.

5. Evolution of β and the Character of ψ

If in a real medium a single transition length λ (measured in the same units as l) can be defined naturally (say, by a characteristic correlation length or fracture segment length), then the ratio λ/l will influence β. Note that λ does not enter the equations in an explicit manner. Rather, we treat the domain under the assumption that λ/l is small enough to allow for the averaging mentioned in section 2 to actually occur. For strong heterogeneity, even with relatively small correlation, this averaging may not be sufficient to permit full mixing. If the ratio λ/l is not sufficiently small and the experimental FPTD curves do not vary smoothly, then the large scale heterogeneities must be treated deterministically.

In fact, β is a function of the length scale (or time needed to traverse this length scale). The CTRW theory development presented here can be applied when β is constant or slowly varying over a number of orders of magnitude in length or time. Geological systems can encounter heterogeneities on different hierarchical scales, and the characteristic length of the largest scale heterogeneity is likely to influence β the most. We note also that for statistically self-similar media, which appears to be the case in at least some geological formations (up to a certain length scale), it can be expected that β will remain constant. On the other hand, if no larger λ appears due to new heterogeneity scales, then for a large enough domain, full averaging will take place and the Gaussian distribution will characterize the tracer plume; i.e., β will increase through the threshold of 2.

We observe for $\beta < 1$ (see section 3) that the mean particle velocity is a decreasing function of the distance traversed by particles. The following simple physical arguments explain this phenomenon. Considering a step injection, faster flow paths will initially be filled faster by particles, i.e., a higher proportion of particles, compared to the carrier liquid, will have higher velocities. In other words, the average particle velocity is higher than that of the carrier liquid. Over time, mixing occurs, and the average particle velocity will decrease. For a pulse injection, if there is a large number of low velocity regions, fast-moving particles may reach the slower flow regions before the slow-moving particles reach the faster flow regions; again, over time, the average particle velocity will decrease.

Particles "sample" the existing velocity field as they migrate through the flow domain. Faster flow regions are sampled more quickly. As the domain size increases, there is more time for particles to sample lower velocity regions. As the number of still lower velocity regions becomes small, the plume velocity

becomes constant. In terms of $\psi(t)$, a small number of regions with low velocity means that $\psi(t)$ will decrease rapidly at long times. In other words, as the distance traveled by particles grows, β increases; when it reaches unity, the mean particle velocity becomes constant and should equal the mean velocity of the carrier liquid. Thus, stating that β increases simply means that with growing domain size, the relevant regions of $\psi(t)$ change.

We note, parenthetically, that the long-time expansions of $\psi^*(u)$ for the special cases of $\beta = 1$ and $\beta = 2$ can be found in ref 9. Here, we do not develop FPTD solutions for these two cases because the probability of encountering these exact values in real geological systems is essentially negligible.

We return now to consider the physical picture of particle transitions discussed in section 2. In accordance with the properties of Lévy distributions (see section 2), it can be seen from (1) that $f(\tau) \sim \tau^{-1-\beta}$ as $\tau \rightarrow \infty$; i.e., the tail drops in exactly the same way as the density function $\psi(t)$ for single displacements. A similar long-time behavior is found in the case $1 < \beta < 2$: we see from (14) that the leading term for $\tau \rightarrow \infty$ is FPTD $\sim h^{-1-\beta} \sim \tau^{-1-\beta}$, as expected.

Thus, this result justifies our choice to work with $\psi(t)$, rather than with an explicitly coupled space−time density function (as discussed in section 2). We emphasize that in the range of a constant β, and since the FPTD is in essence the transition time density for a displacement interval of length L, theoretical predictions using the CTRW are not a function of the prescribed single displacement length. Moreover, modeling particle movement by considering coupled transition time distributions for different distances will not affect the predictions. Further aspects of the relationships between coupled and uncoupled formulations of the transition probability functions are currently under investigation.

6. Summary and Conclusions

In this work the physical basis of CTRW theory and its relevance to modeling transport in heterogeneous geological formations was discussed. In view of the different heterogeneity scales, it seems natural to apply this approach. The CTRW considers transport phenomena on "small" scales, where global averaging cannot be applied (although in terms of geological formations, "small" can be of the order of hundreds of meters, or more). While typical homogenization methods are generally applicable only for mildly heterogeneous systems, the CTRW is especially powerful for strongly heterogeneous media.

We present new theoretical results for the FPTD in the important case $1 < \beta < 2$, where β is the central parameter of CTRW theory, and show that for $\beta > 2$ the Gaussian distribution is recovered. As a consequence, the entire possible range of β values and transport behaviors is discussed. Finally, a method to compare the theoretical FPTD solutions to experimental measurements is described.

Acknowledgment. We thank Harvey Scher for many useful discussions and for a critical reading of this manuscript. We acknowledge the financial support of the European Commission (Contract ENV4-CT97-0456).

References and Notes

(1) Bear, J. *Dynamics of Fluids in Porous Media*; American Elsevier Publishing Co., Inc.: New York, 1972.
(2) Dagan, G., Neuman, S. P., Eds. *Subsurface Flow and Transport: A Stochastic Approach*; Cambridge University Press: Cambridge, U.K., 1997.
(3) Scher, H.; Lax, M. *Phys. Rev. B* **1973**, *7* (10), 4491.
(4) Scher, H.; Lax, M. *Phys. Rev. B* **1973**, *7* (10), 4502.
(5) Montroll, E. W.; Scher, H. *J. Stat. Phys.* **1973**, *9* (2), 101.
(6) Scher, H.; Montroll, E. W. *Phys. Rev. B* **1975**, *12* (6), 2455.
(7) Berkowitz, B.; Scher, H. *Phys. Rev. E* **1998**, *57* (5), 5858.
(8) Berkowitz, B.; Scher, H.; Silliman, S. E. *Water Resour. Res.* **2000**, *36* (1), 149.
(9) Shlesinger, M. F. *J. Stat. Phys.* **1974**, *10* (5), 421.
(10) Shlesinger, M. F.; Zaslavsky, G. M.; Klafter, J. *Nature* **1993**, *363*, 31.